View metadata, citation and similar papers at core.ac.uk

brought to you by CORE

provided by NASA Technical Reports Server

U. of Iowa 67-18

MICROBURST PHENOMENA

1. Auroral Zone X-rays*

by

D. Venkatesan
Department of Physics
The University of Calgary
Calgary, Alberta, Canada

M. N. Oliven[1]
Department of Physics and Astronomy
University of Iowa
Iowa City, Iowa, USA

and

P. J. Edwards,[2] K. G. McCracken[2] and M. Steinbock[3]
Southwest Center for Advanced Studies
Dallas, Texas, USA

September 1967

* Work at The University of Calgary by National Research Council grant A-3865, at the University of Iowa by Office of Naval Research Contract 1509(06), and at the Southwest Center for Advanced Studies by NASA Contract NASr-198.

[1] NASA Graduate Trainee

[2] Current Address: Physics Department, University of Adelaide, Adelaide, South Australia

[3] Address 1966-67: Physics Department, The University of Calgary, Calgary, Alberta, Canada

ABSTRACT

High-time resolution x-ray equipment flown from Ft. Churchill, Manitoba, Canada on August 11, 1965 provides evidence for species of auroral zone x-ray microbursts with an asymmetric time profile. These asymmetric microbursts are characterized by a rise of the form $1 - e^{-t/\tau_R}$ where τ_R is about 30 milliseconds, and a decay of the form of e^{-t/τ_D} where τ_D is about 200 milliseconds, and a typical peak flux for the largest events of J_o ($E_{x\text{-ray}} > 60$ keV) $\sim 10^2$ photons cm^{-2} sec^{-1} at $10\,g/cm^2$. An episode of these asymmetric bursts was observed in the early morning hours (after 4:30 local time) and an episode of the more common symmetric microbursts began after 9:30 local time. The fast rise times, and the lack of dispersion $\gtrsim 10$ milliseconds in the x-ray bursts observed at different energies implies restrictions on the nature, and propagation of the parent electron microbursts.

INTRODUCTION

Numerous rocket and balloon studies in the auroral zone have investigated the bremsstrahlung x-radiation produced by electrons impinging upon the upper atmosphere. With the availability of data from charged particle detectors on polar satellites, measuring precipitated electrons, it is now possible to investigate the behavior of both the parent electrons and the daughter bremsstrahlung x-rays.

This study reports on a portion of the data obtained during a series of seven balloon flights made from Fort Churchill, Canada, of balloon-borne scintillator-photomultiplier x-ray detectors. The geographic coordinates of the balloon launch site are 58.75°N and 94.09°W (L = 8.66). The data of interest herein, were obtained during a balloon flight which commenced at 0225 UT on August 11, 1965, during a period of relatively low geomagnetic activity. The International Planetary Index for geomagnetic activity, K_p, was 1_o or less during the entire flight period.

The balloon reached a ceiling altitude of 110,000 feet at 2315 local time (0515 UT) and thereafter drifted in a west-southwesterly direction. It remained above 106,000 feet during the period of 15 hours, during which useful data were acquired at the

telemetry receiving station. Table 1 gives the positions of the balloon during the period of interest, namely 0700-1700 UT (0100-1100 LT) and the L coordinate corresponding to the positions. Also given, for comparison, are the L values for places from which other x-ray experiments have been flown before.

INSTRUMENTATION

The detection system, illustrated in Figure 1, consisted of a 5 inch diameter, half inch thick NaI(Tl) scintillation crystal, viewed by a Dumont 6364 photomultiplier of the same diameter. The geometric factor of the detector for x-rays isotropic over the whole of the upper hemisphere, was 476 cm^2ster. A lucite light pipe, of the same dimensions as the crystal, separated the crystal and the phototube by 2 cm, in order to minimize the effects of photocathode non-uniformities upon the energy resolution of the system.

The photomultiplier EHT was supplied from a regulated DC converter, which in turn obtained its power from a series of mercury batteries. The whole high voltage system was vacuum potted to eliminate the possibility of corona. A μ-metal shield enclosed the photomultiplier dynode chain and the photocathode, and this minimized the perturbation of the electron orbits and hence the photomultiplier gain, by the earth's magnetic field. The complete detector system was observed to yield a resolution of 50% FWHM for the 32 keV x-ray from Cs^{137}.

After linear pulse amplification, the photomultiplier pulses were applied to a three window pulse height analyzer, with contiguous windows set to 20-40 keV, 40-60 keV, and > 60 keV. The energy calibration of each window was adjusted, prior to flight, using known monochromatic x-ray sources, and a 400 channel pulse height analyzer operating in the coincidence mode. Each of the outputs from the three window pulse height analyzer was fed to identical logarithmic count-rate meters, and also to a three position subcommutator which sampled each of the three pulse rates for a minute at a time. The output from the subcommutator was fed to a binary scaler with outputs at scaling factors of 64 and 1024. The counting rate meter outputs, and the two scaler outputs were fed to separate FM subcarrier oscillators, which were used to modulate the telemetry transmitter, delivering a power of 0.25 watts into a vertically polarized coaxial sleeve antenna at 72 mc/sec.

The response time of the counting rate meter circuits was determined to be 3 milliseconds for an instantaneous increase in pulse input rate. Each count rate meter was individually calibrated prior to flight, and the two binary scaler outputs

were used to provide an inflight check of the calibrations. An inflight calibration of the subcarrier oscillator stability was also provided by sampling a stabilized square wave input periodically throughout the flight.

OBSERVATIONS

The first six hours of x-ray data obtained after the balloon attained ceiling altitude were rather featureless. Beginning at 1028 UT (0428 LT) and over a period of 6-1/2 hours, however, the data revealed a great variety and number of fast time variations of auroral zone x-ray activity. The magnetometer records at Fort Churchill showed no appreciable magnetic activity during this period, nor did the riometer register any event. Since these x-ray events occurred during daylight hours, no visual confirmation of the presence of aurorae was possible.

Figures 2 and 3 presents a number of typical fast rise-time x-ray bursts. They appear in large numbers, both as isolated events emerging from the background and in trains occurring in close succession with an apparent periodicity of approximately 0.6 second. When two follow each other very closely, the result is a compound structure in which the two leading edges can usually be discerned. Furthermore, there are also periods of complex activity during which the absolute x-ray flux is so high that any attempt at isolation of such bursts is futile, although

one does see indications of the superposition of individual bursts. The overall features of these bursts are, in general, similar to those that have been reported and discussed previously by Anderson and Milton [1964] and Anderson [1965], who have named them microbursts, Parks [1967], and several other authors. In view of the fact that the bursts observed during the flight reported herein are also devoid of substructure and are of the same time scale, we adopt the same terminology of microbursts, since there is enough general evidence to show that the bursts herein described belong to the same general category of those observed by Anderson and Milton [1964].

The microbursts activity appears in two time intervals, separated by 1-3/4 hours of little activity, the two periods containing bursts having significantly different characteristics. During the earlier epoch of activity, 1027-1355 UT (0427-(0755 LT), the bursts have hard spectra, very fast rise times and slower decay times and, as such, are somewhat different from the more symmetric microbursts discussed by earlier authors. Thr original recognition of these asymmetric bursts represents the first time that such asymmetric microbursts have been reported (Edwards et al. [1966]). Later, during the period

1540-1707 UT (0940-1107 LT), the character of the observed microbursts is essentially symmetric, the events exhibiting characteristics similar to the microbursts reported by Anderson and Milton [1964]. An example of each of the two types, together with one of less severe asymmetric features (an intermediate type) observed in the late morning, is presented in Figure 4.

Preceding the initial onset of the period of microburst activity, a gradual increase in the background counting rate of the 20-40, 40-60, and > 60 keV energy channels was observed. Such increases prior to microburst epochs have also been reported by Anderson and Milton [1964]. It should be pointed out that the peak intensities of the asymmetric bursts observed by us are similar to those of the symmetric ones seen by Anderson and his co-workers. In common with them, more than half the peak fluxes were less than 20 cm^{-2} sec^{-1} above background and only about one percent of the asymmetric bursts had peak fluxes in excess of 60 cm^{-2} sec^{-1} at an atmospheric depth of 10 g/cm^2.

Certain gross features of the x-ray events emerge from a general study of the entire data. The occurrence of asymmetric microbursts is seldom isolated, but continues over an extended period of time. There seems to be no evident relationship

between the onset of the asymmetric microbursts and the nature of the preceding x-ray activity. In short, the onset of these microbursts appears to be sudden and impulsive. It is observed that the asymmetric bursts are more predominant in the $E > 60$ keV channel than are the symmetric bursts, indicative of a harder photon spectrum. A peak flux above previous background level of $J_o(E > 60 \text{ keV}) \approx 10^2$ photons cm^{-2} sec^{-1} can be observed in the $E > 60$ keV channel during a large asymmetric event. The individual microbursts maintain their identity (i.e. the rise and decay times are not changed) despite superposition upon one another, or upon a smooth background of x-ray activity. The shortness of the characteristic times of the microbursts, especially the asymmetric variety, would appear to be of importance in the understanding of the dynamic processes responsible for the parent precipitation phenomenon. A logical step forward would be to investigate the parent particle precipitation, using detectors on high latitude satellites, and this has been done and is discussed in a companion paper (Oliven, et al. [1967]).

The present study reveals a wide variability in the rise time characteristics of x-ray microbursts. The asymmetric microbursts observed during early morning hours are characterized by rise times, τ_R of about 20-30 milliseconds and by decay times, τ_D of

about 200 milliseconds where the rising and decay phases are represented by $(1 - e^{-t/\tau_R})$ and e^{-t/τ_D}, respectively. Throughout the period of activity, one feature noticed was that the time of apparent duration of a burst, namely the period during which it is visible above background from the rise to the apparent end of the decay, was almost always between 300 and 500 milliseconds. This feature is in agreement with a similar characteristic of the symmetric bursts observed by Anderson and Milton [1964] whose flights were from Flin Flon at L = 6.1.

One hundred of the large asymmetric bursts were studied in detail, the frequency distribution of rise times for these events being given in Figure 5. About 60% of the cases have rise times $\leq$ 50 milliseconds. A composite of 75 of these microbursts is shown in Figure 6, and a decay time constant of 200 milliseconds is apparent. Figure 7, an example of an individual burst, shows a rise time of 30 milliseconds and a decay time of 200 milliseconds. The $E > 60$ keV energy window is displayed in all these diagrams.

Figure 8 gives samples of all three energy channels during the late morning hours when symmetric bursts were seen. Anderson, et al.

[1966] have also made flights recently at L ~ 8.0, but they have observed predominantely the symmetric type of bursts during their flights. Although one does see the asymmetric bursts occasionally in the lower energy channels, it is possible to generalize that, in most of the examples of asymmetric microbursts observed during our flight, the highest energy channel contained the highest counting rate of all the channels (see Figure 3). The symmetric bursts, on the other hand, were observed to exhibit comparable responses in all three channels.

To study the photon energy spectrum of the asymmetric microburst, we have computed the ratios of counting rates, above background of:

$$\frac{\text{x-rays, energy} > 40 \text{ keV}}{\text{x-rays, energy} > 60 \text{ keV}}, \qquad \frac{\text{x-rays, energy} > 20 \text{ keV}}{\text{x-rays, energy} > 60 \text{ keV}}, \qquad \text{and}$$

$$\frac{\text{x-rays, energy} > 20 \text{ keV}}{\text{x-rays, energy} > 40 \text{ keV}}$$

at 10 millisecond intervals, throughout the entire duration of individual bursts. Figure 9 shows the largest observed burst, with the analog output at the top, and the ratios at the bottom. The

ratios have the lowest values within 10 milliseconds of the occurrence of peak counting rates in all three channels, and this indicates relatively small dispersions ($\leq$ 10 milliseconds) in the arrival of the parent precipitating particles of different energies at the production layer.

Although our emphasis in this paper has been on the newly observed fast rising asymmetric microbursts, nevertheless, it is worthwhile to make some comparison with the better known types of symmetric bursts, observed by us during the latter half of the flight. A frequency distribution of the rise times for both types of events is presented in Figure 10, and it can be seen that there is no prominent peaking in the lower histogram; that is, the rise times of the symmetric microbursts display a wide variability. Specifically, only 22% of the symmetric events have rise times $\leq$ 50 milliseconds in contrast to 71% in the case of asymmetric events.

Figures 11 and 12 display composite asymmetric and symmetric microbursts for the energy ranges 40-60 keV, and $>$ 60 keV, and it can be seen that the symmetric microburst clearly possesses the softer spectrum of the two species of events. The e-folding energies for both types of events are significantly

higher than those obtained in the vicinity of $L \approx 5$ to 6 by other investigators. The composite asymmetric burst spectrum has an e-folding energy, $E_o \sim 360$ keV at peak intensity. The spectrum slowly softens with E_o falling to $\sim$ 200 keV near the end of the events. The spectrum of the symmetric bursts hardens during the rise to peak intensity, at which time $E_o \sim 160$ keV and this softens with E_o eventually falling below 60 keV. In both cases the event spectra are substantially harder than that of the background radiation. It must be remembered here, that with such large values for E_o and in consideration of the restrictions which a limited two or three point determination of E_o impose, the true significance of these e-folding energies is lost. The values stated are just presented to give a numerical answer and do not necessarily imply a spectrum of this form, characterized by these values of E_o.

SUMMARY AND CONCLUSIONS

The primary object of the study has been the investigation of auroral zone x-ray microbursts, with high-time resolution balloon-borne equipment at high latitudes (magnetic shell parameter $L \sim 8$). These balloon results are presented herein, and those correlating the x-ray microbursts with satellite observations are presented in the following companion paper (Oliven, et al. [1967]). A third paper (Oliven and Gurnett [1967]), establishing a connection between microbursts and VLF phenomena also follows.

A new type of microburst has been observed and reported herein with the characteristics of a hard energy spectrum, fast rise time, of order 30 milliseconds, and a decay of time constant $\sim$ 200 milliseconds. Symmetric microbursts, similar in time structure to those reported by others were also observed during the latter half of the flight. The latter occurred at a slightly lower L value and at a later time, (local time 9:30 in contrast with 4:30), than the asymmetric microbursts.

The asymmetric microbursts have a harder spectrum than the symmetric events, as is evidenced by the large response in the high energy channel ($E > 60$ keV) as compared to that in the lower channels. In contrast, the symmetric bursts are characterized by comparable responses in the lower energy channels (20-40 and 40-60 keV). A typical peak flux for the asymmetric events in the > 60 keV channel is given by $J_o(E_{x\text{-}ray} > 60 \text{ keV}) \approx 20$ photons cm^{-2} sec^{-1}.

The extremely hard photon spectra found for the larger events, (e-folding energies of the order of hundreds of keV) place rather stringent instructions on the interpretation of the events. If the precipitating particles responsible for these symmetric and asymmetric bursts are assumed to be electrons, then the x-ray spectra must be scrutinized in terms of the differential energy spectra of the parent electrons, within the restrictions imposed by the range of the three channels and the two or three point determination of the x-ray spectra. It appears necessary to postulate relativistic electrons with an insignificant flux at lower energies. Differential electron spectra with a high energy peak > 400 keV have been deduced by Mozer and Bruston [1966] and rapid fluctuations in the integral

flux above 400 keV have been seen by Blake, et al. [1966], and the impulsive bursts reported herein may be an extension of these relativistic electron populations.

The spectra of the harder asymmetric bursts is not as easily interpreted in terms of electron bremsstrahlung radiation. One of the possible explanations could be that of the proton-excited gamma radiation. If the events were due to proton-excited gamma radiation (Hoffmann and Winckler, [1961]) then no special assumptions about the proton energy spectrum are necessary. As an example, a flux of $\sim 10^5$ protons cm^{-2} sec^{-1} above 0.5 MeV (the Injun 3 geiger counter threshold) having a differential power law spectral index of -5 could account for the larger asymmetric bursts. These protons might augment the precipitating electron population. At the present time, we have no direct evidence for the contribution protons may make in the production of these asymmetric x-ray microbursts.

To summarize, the detailed study of the newly observed asymmetric x-ray microbursts, in addition to the better known symmetric microbursts, has provided a supplement to the knowledge of fast temporal variations in auroral zone x-rays. The fast rise times and hard spectra impose rather stringent conditions on the mechanisms involved in this impulsive particle precipitation,

and in turn upon the causative plasma instabilities within the magnetosphere. In particular, we note that the asymmetric microburst indicates dipersion times of < 10 milliseconds for the particles responsible for the microburst, implying either a limit on the distance from the source particle to the earth, or that there is a significant particle-particle or particle-field interaction, so that the particles remain bunched while propagating through the geomagnetic field.

ACKNOWLEDGMENTS

The authors wish to express their thanks for the advice and support offered in this project by Professor J. A. Van Allen of the University of Iowa. This work was supported at The University of Calgary by National Research Council Grant A-3865, at the University of Iowa by Office of Naval Research Contract 1509(06), and at the Southwest Center for Advanced Studies by NASA Contract NAS-r-198. We wish to acknowledge substantial design contributions made by Messrs. C. Adair and L. Brooks, and the assistance of the various personnel associated with the ONR Skyhook expedition of 1965.

REFERENCES

Anderson, K. A., "Balloon Measurements of X-rays in the Auroral Zone," Auroral Phenomena, ed. M. Walt (Stanford University Press, Stanford, California), 1965.

Anderson, K. A., L. M. Chase, H. S. Hudson, M. Lampton, D. W. Milton, and G. P. Parks, "Balloon and Rocket Observations of Auroral Zone Microbursts," J. Geophys. Res. 71, 4617-4629 (1966).

Anderson, K. A., and D. W. Milton, "Balloon Observations of X-rays in the Auroral Zone. 3. High Time Resolution Studies," J. Geophys. Res. 69, 4457-4479 (1964).

Blake, J. B., S. C. Freden, and G. A. Paulikas, "Precipitation of 400 keV Electrons in the Auroral Zone", J. Geophys. Res. 71, 5129-5134 (1966).

Edwards, P. J., K. G. McCracken, M. Steinbock, M. Oliven, and D. Venkatesan, "Impulsive Precipitation of Electrons in the Auroral Zone," Trans. Am. Geophys. Union 47, 139 (1966).

Hoffmann, D. J. and J. R. Winckler, "Simultaneous Balloon Observations at Fort Churchill and Minneapolis during the Solar Cosmic Ray Events of July 1961", J. Geophys. Res. 68, 2067-2098 (1963).

Mozer, F. S. and P. J. Bruston, "Properties of the Auroral Zone Electron Source Deduced from Electron Spectrums and Angular Distributions," J. Geophys. Res. 71, 4451-4460 (1966).

Oliven, M. N., D. Venkatesan, and K. G. McCracken, "Microburst Phenomena. 2. Auroral Zone Electrons", U. of Iowa 67-19 (submitted to J. Geophys. Res. for publication).

Oliven, M. N. and D. A. Gurnett, "Microburst Phenomena. 3. An Association Between Electron Microbursts and VLF Chorus", U. of Iowa 67-39 (submitted to J. Geophys. Res. for publication).

Parks, G. K., "Spatial Characteristics of Auroral-Zone X-ray Microbursts," J. Geophys. Res. 72, 215-226 (1967).

TABLE 1

Location		Latitude	Longitude	L Value
		Balloon at:		
700 UT		58.50	266.20	8.457
800 UT		58.50	265.90	8.426
900 UT		58.50	265.30	8.362
1000 UT		58.30	265.10	8.192
1100 UT		58.30	264.50	8.128
1200 UT		58.30	263.90	8.064
1300 UT		58.40	263.40	8.081
1400 UT		58.40	262.90	8.025
1500 UT		58.40	262.30	7.957
1600 UT		58.40	261.80	7.969
1700 UT		58.50	261.20	7.897
Kotzebue, Alaska	(1)	66.90	197.50	5.208
Kiruna, Sweden	(1)	67.80	20.40	5.417
College, Alaska	(1)	66.90	197.50	5.208
Flin Flon, Manitoba	(2)	56.00	258.00	6.120
Ft. Yukon, Alaska	(1)	66.60	214.70	6.468
Pt. Barrow, Alaska	(1)	71.50	203.70	8.263
Ft. Churchill, Manitoba	(2)	58.80	265.90	8.660

(1) Indicates low time resolution equipment flown from these points

(2) Indicates fast time resolution equipment flown from these points.

FIGURE CAPTIONS

Figure 1 Block diagram of the entire system associated with the x-ray detector.

Figure 2 Typical appearance of fast-rise time x-ray microbursts. In the top data-segment compound events are seen, whereas in the bottom two examples combs or trains and single bursts can be identified. Vertical scales of bursts are analog.

Figure 3 Two examples of asymmetric microbursts as they appear, singly, in all three energy channels. All vertical scales of bursts are analog.

Figure 4 Comparison of the asymmetric microbursts seen in the early morning hours, a more symmetric type of burst seen later in the morning and the symmetric type of microburst seen late in the morning and similar to the type commonly observed by other experimenters (e.g., Anderson and Milton [1964]). The lower two bursts have been normalized to the top burst.

Figure 5 Distribution of rise times for 100 large asymmetric microbursts.

Figure 6 Composite time profile of 75 individually analyzed asymmetric microbursts.

Figure 7 Time profile of a typical large asymmetric microburst revealing the characteristic time constants.

Figure 8 The appearance in three energy channels of the symmetric microburst species observed late in the morning, August 11, 1965. Vertical scales are analog.

Figure 9 Largest observed asymmetric microburst for three energy windows and the ratios between the various energy channels. Vertical scale of burst is analog.

Figure 10 Comparison between the distribution of rise times for asymmetric and symmetric microbursts.

Figure 11 Comparison curves of the energy channels $E > 60$ keV and $40 \text{ keV} \leq E \leq 60$ keV for 25 asymmetric microbursts.

Figure 12 Composite curves of the energy channel $E > 60$ keV and $40 \text{ keV} \leq E \leq 60$ keV for 25 symmetric microbursts.

G66-200

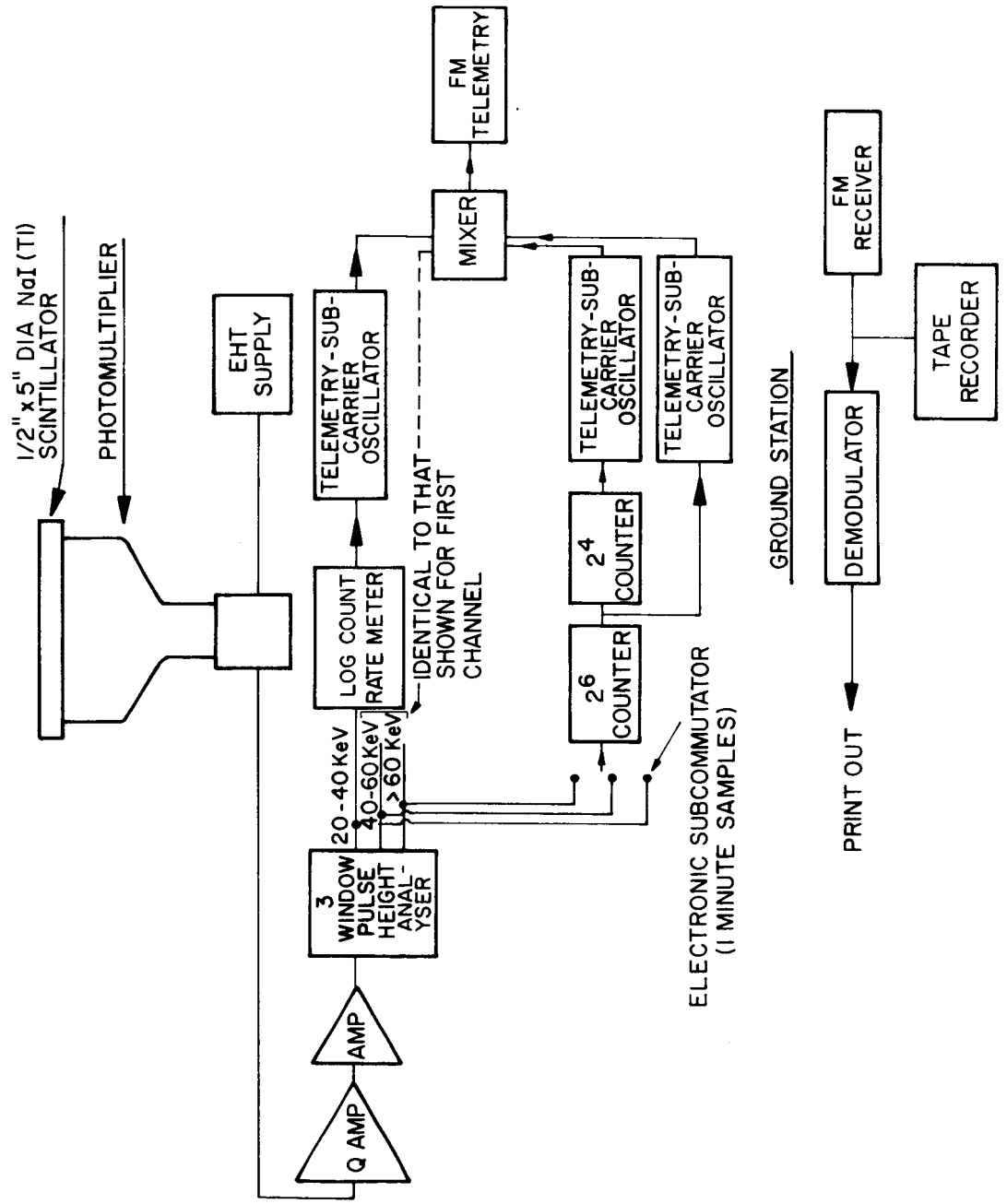

FIGURE 1

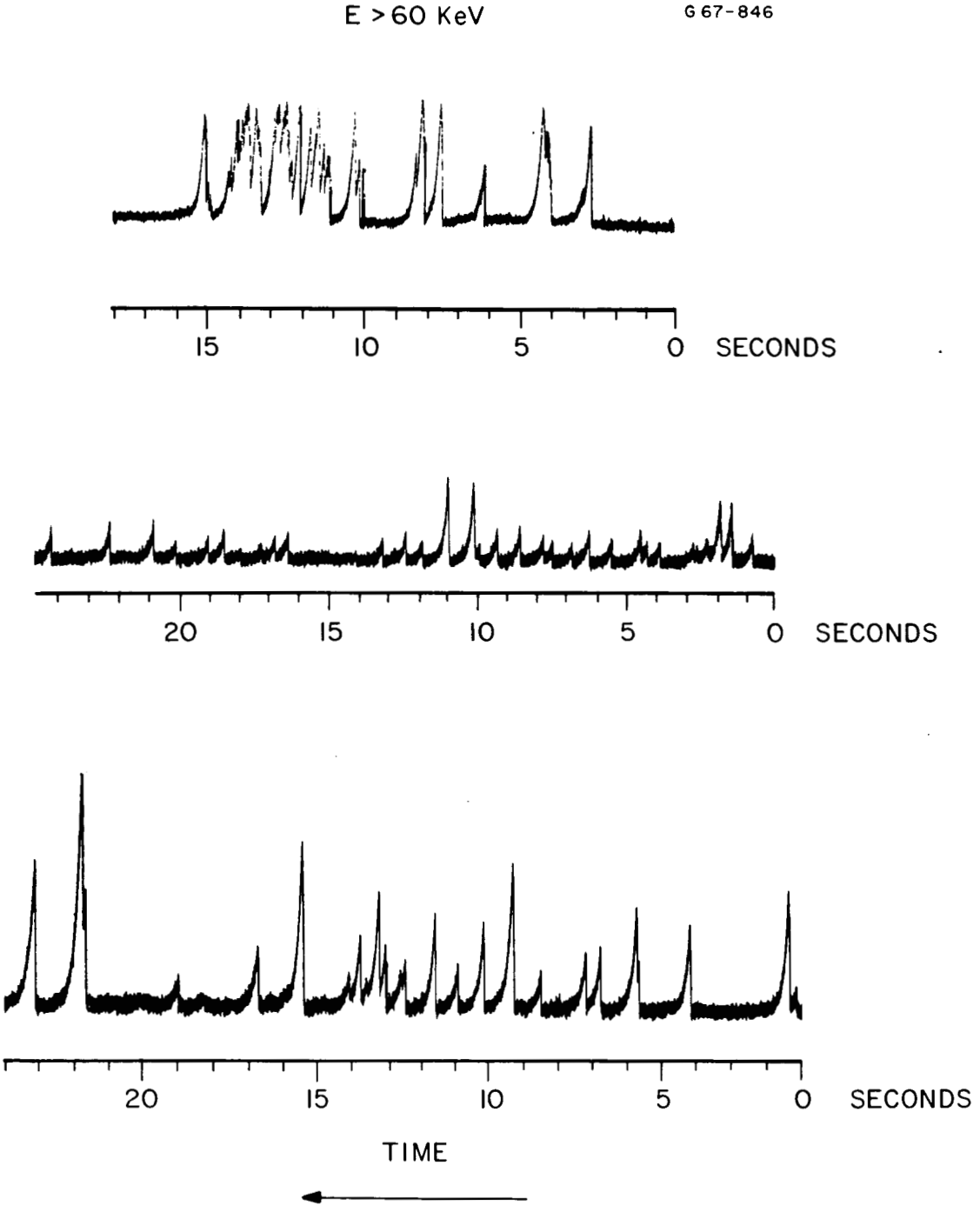
E > 60 KeV
G 67-846
15
10
5
0
SECONDS
20
15
10
5
0
SECONDS
20
15
10
5
0
SECONDS
TIME

FIGURE 2

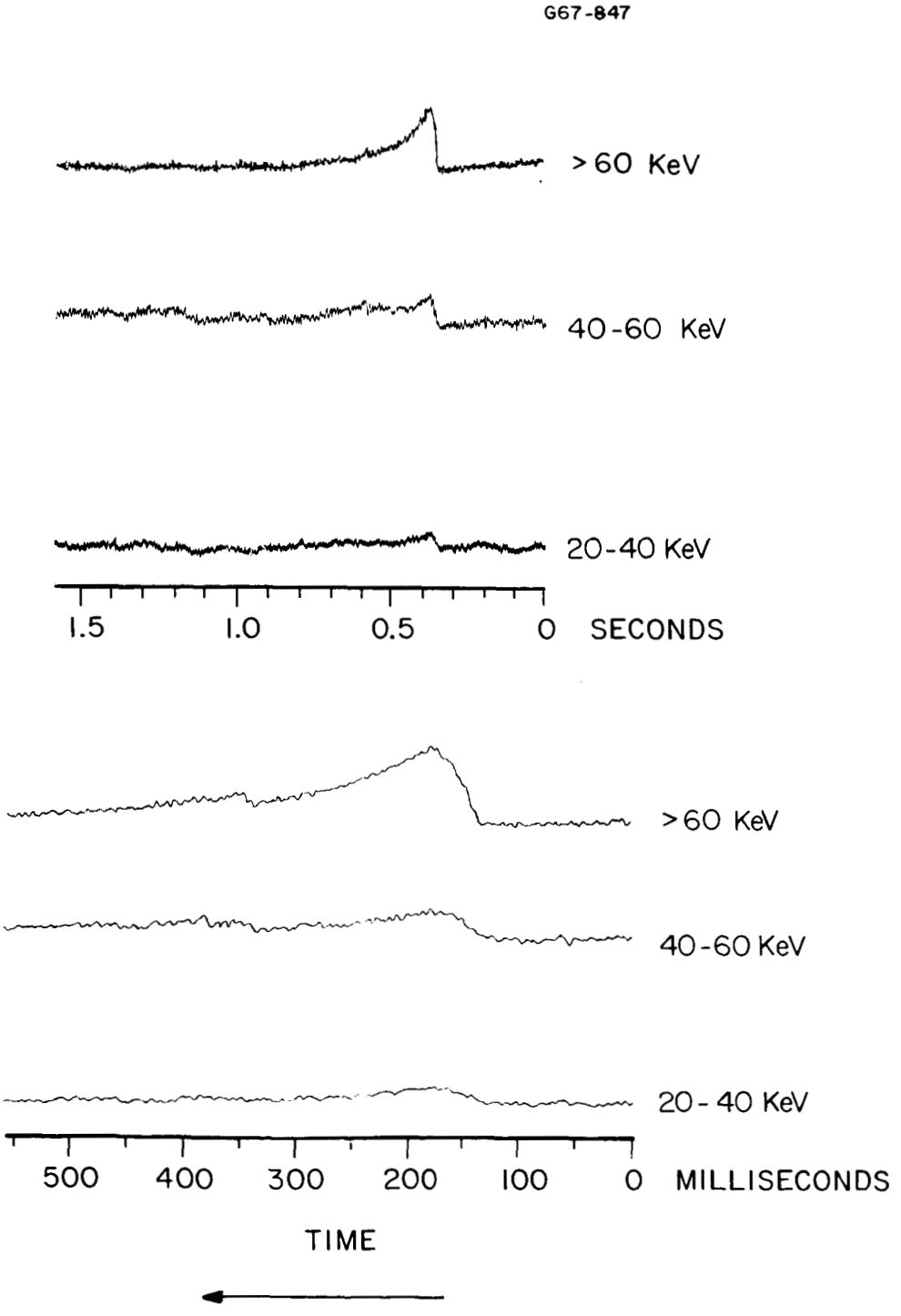
G67-847
>60 KeV
40-60 KeV
20-40 KeV
1.5
1.0
0.5
0
SECONDS
>60 KeV
40-60 KeV
20-40 KeV
500
400
300
200
100
0
MILLISECONDS
TIME

FIGURE 3

G 67-128 (R-1)

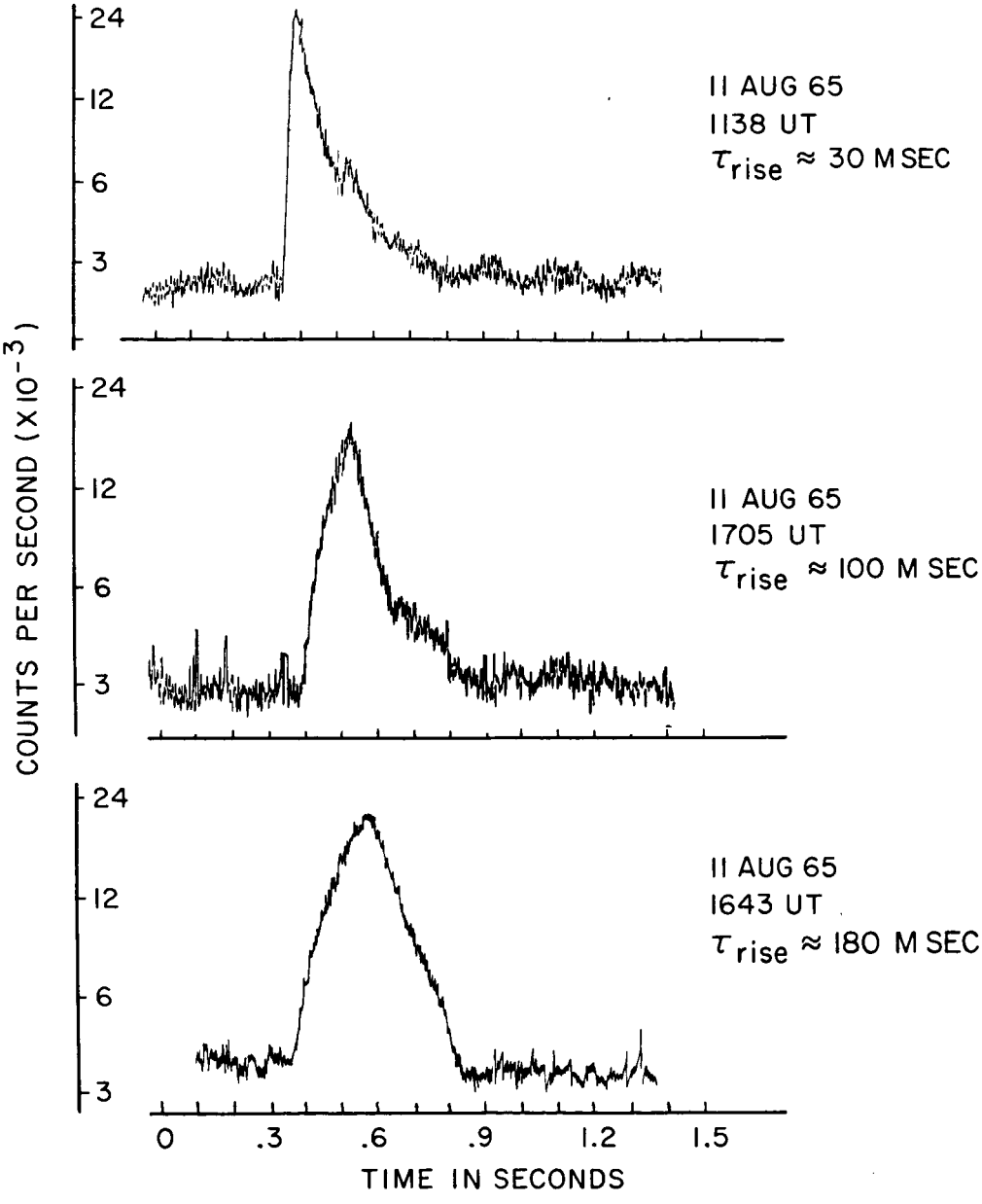

FIGURE 4

G 66-346

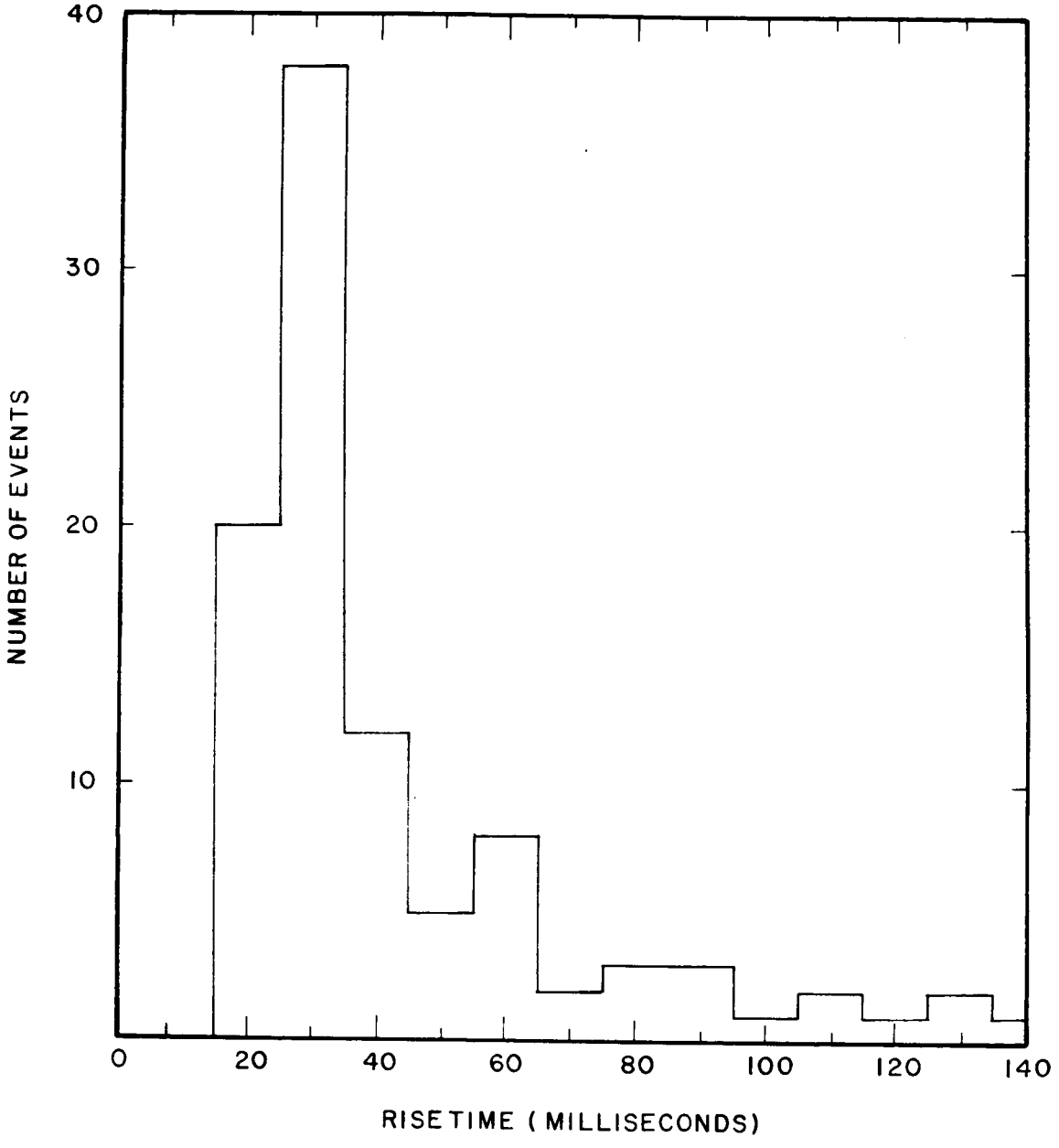

FIGURE 5

G 66-345

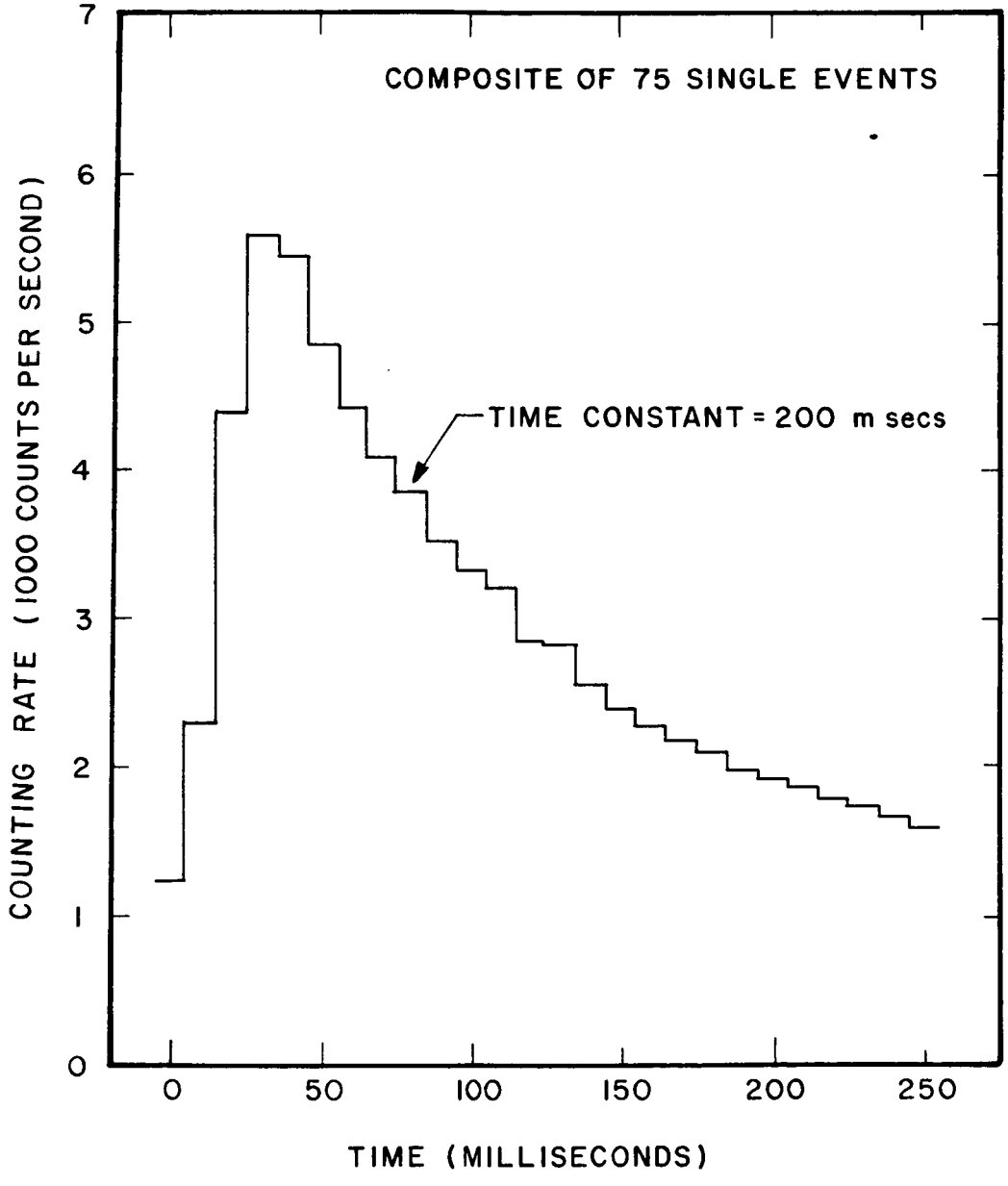

FIGURE 6

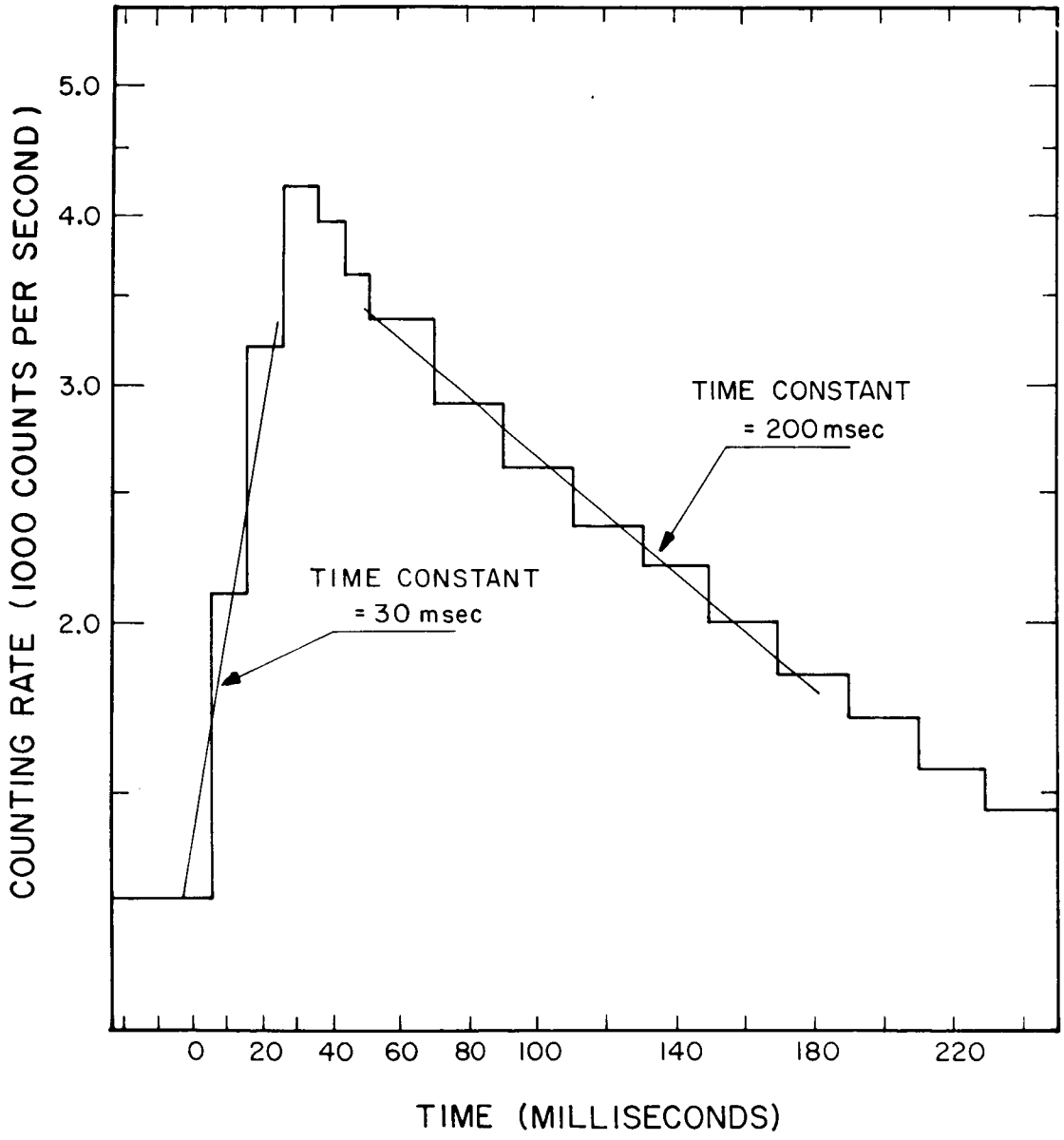
COUNTING RATE (1000 COUNTS PER SECOND)
5.0
4.0
3.0
2.0
TIME CONSTANT
= 200 msec
TIME CONSTANT
= 30 msec
0
20
40
60
80
100
140
180
220
TIME (MILLISECONDS)

FIGURE 7

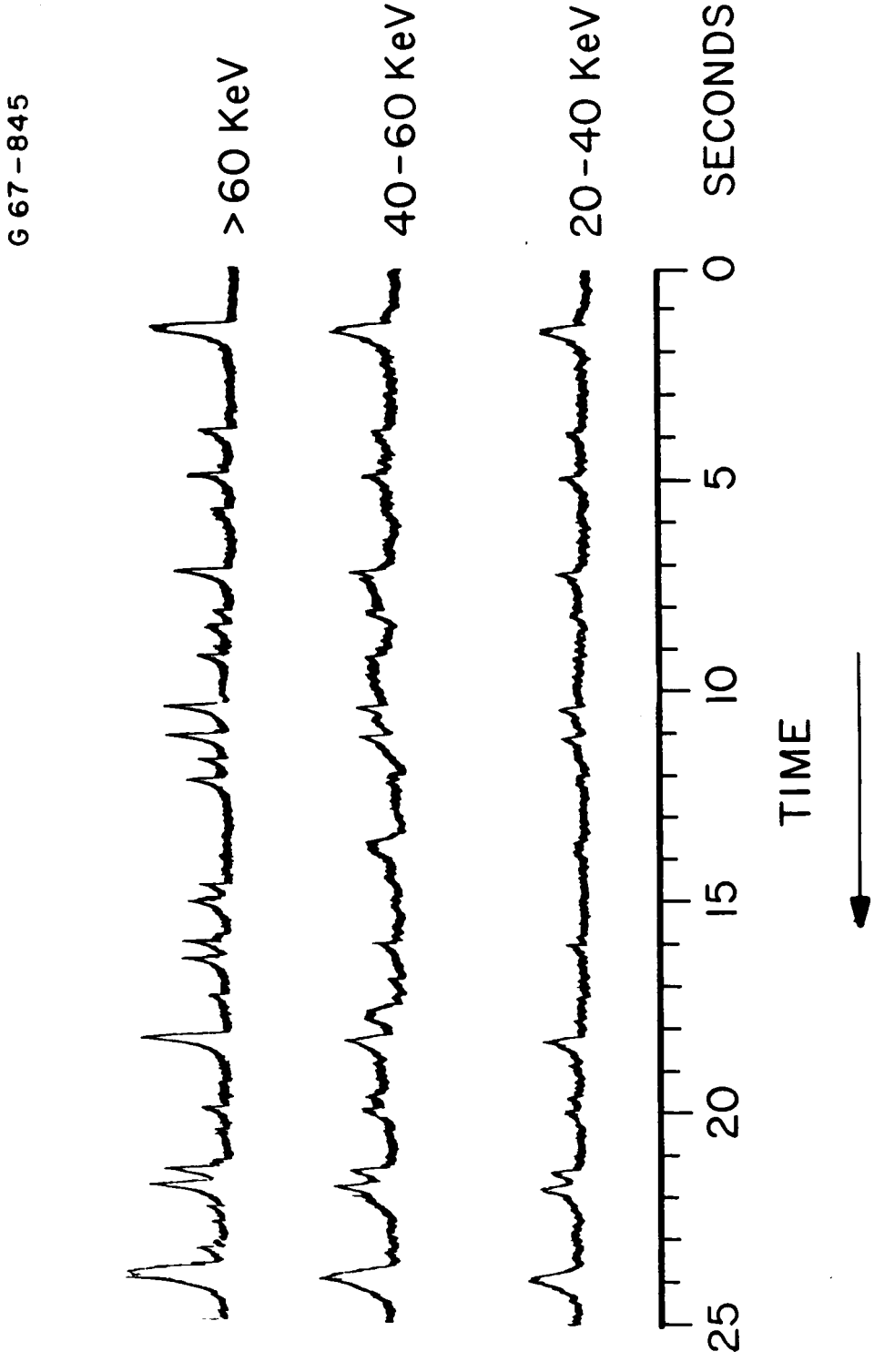

FIGURE 8

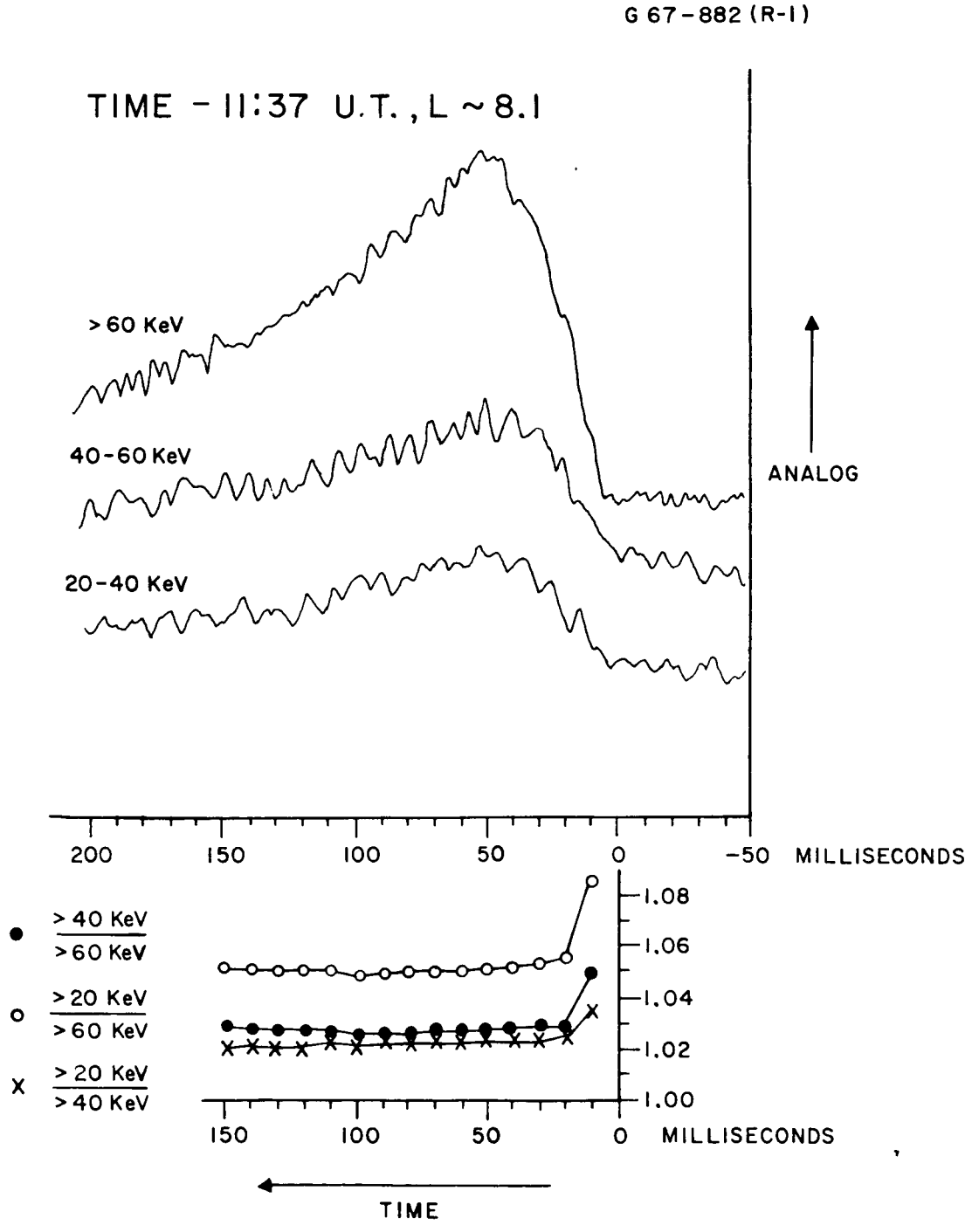
G 67-882 (R-1)
TIME - 11:37 U.T., L ~ 8.1
> 60 KeV
40-60 KeV
20-40 KeV
ANALOG
200
150
100
50
0
-50
MILLISECONDS
> 40 KeV / > 60 KeV
> 20 KeV / > 60 KeV
> 20 KeV / > 40 KeV
1.08
1.06
1.04
1.02
1.00
150
100
50
0
MILLISECONDS
TIME

FIGURE 9

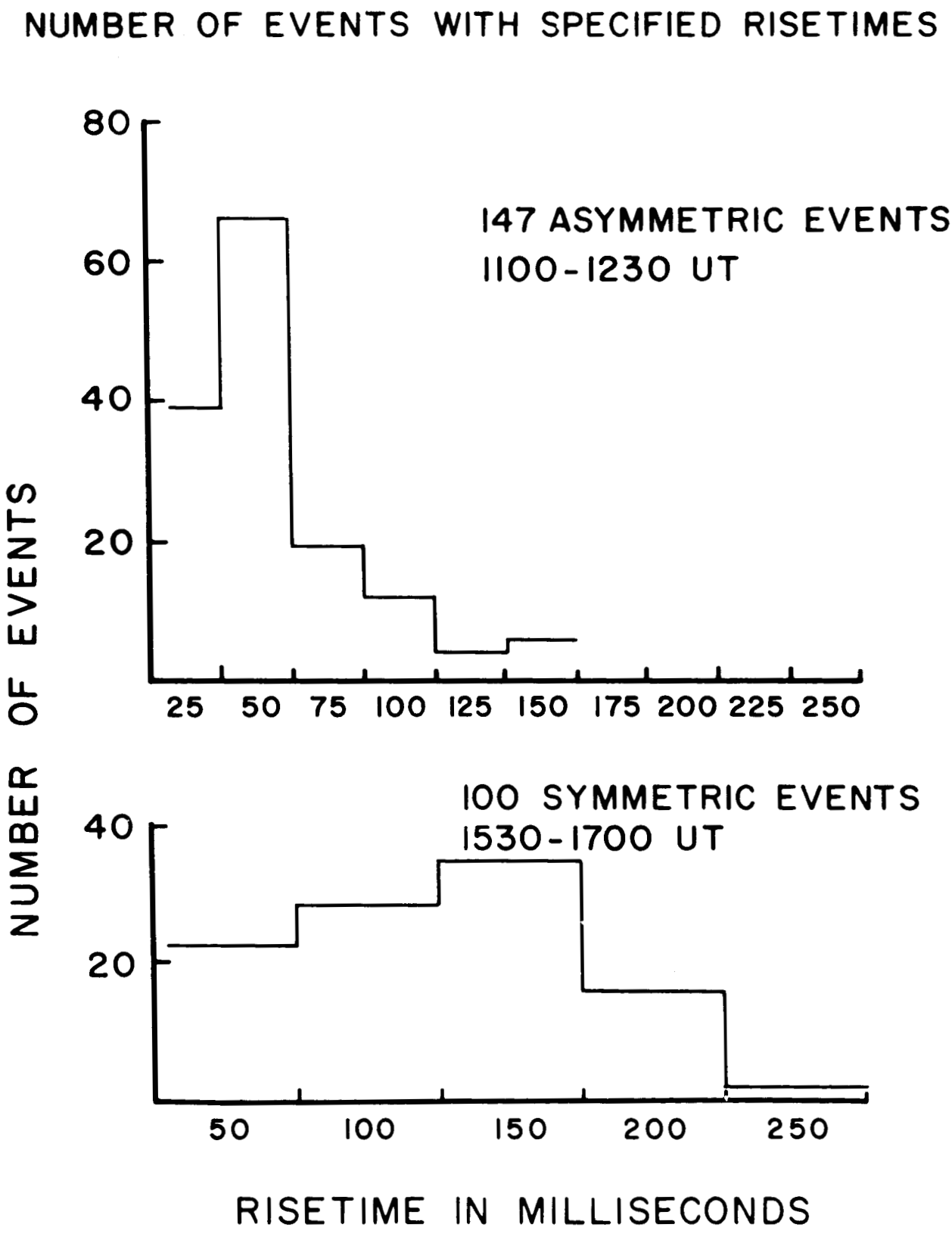
NUMBER OF EVENTS WITH SPECIFIED RISETIMES
80
60
40
20
147 ASYMMETRIC EVENTS
1100-1230 UT
25 50 75 100 125 150 175 200 225 250
NUMBER OF EVENTS
40
20
100 SYMMETRIC EVENTS
1530-1700 UT
50 100 150 200 250
RISETIME IN MILLISECONDS

FIGURE 10

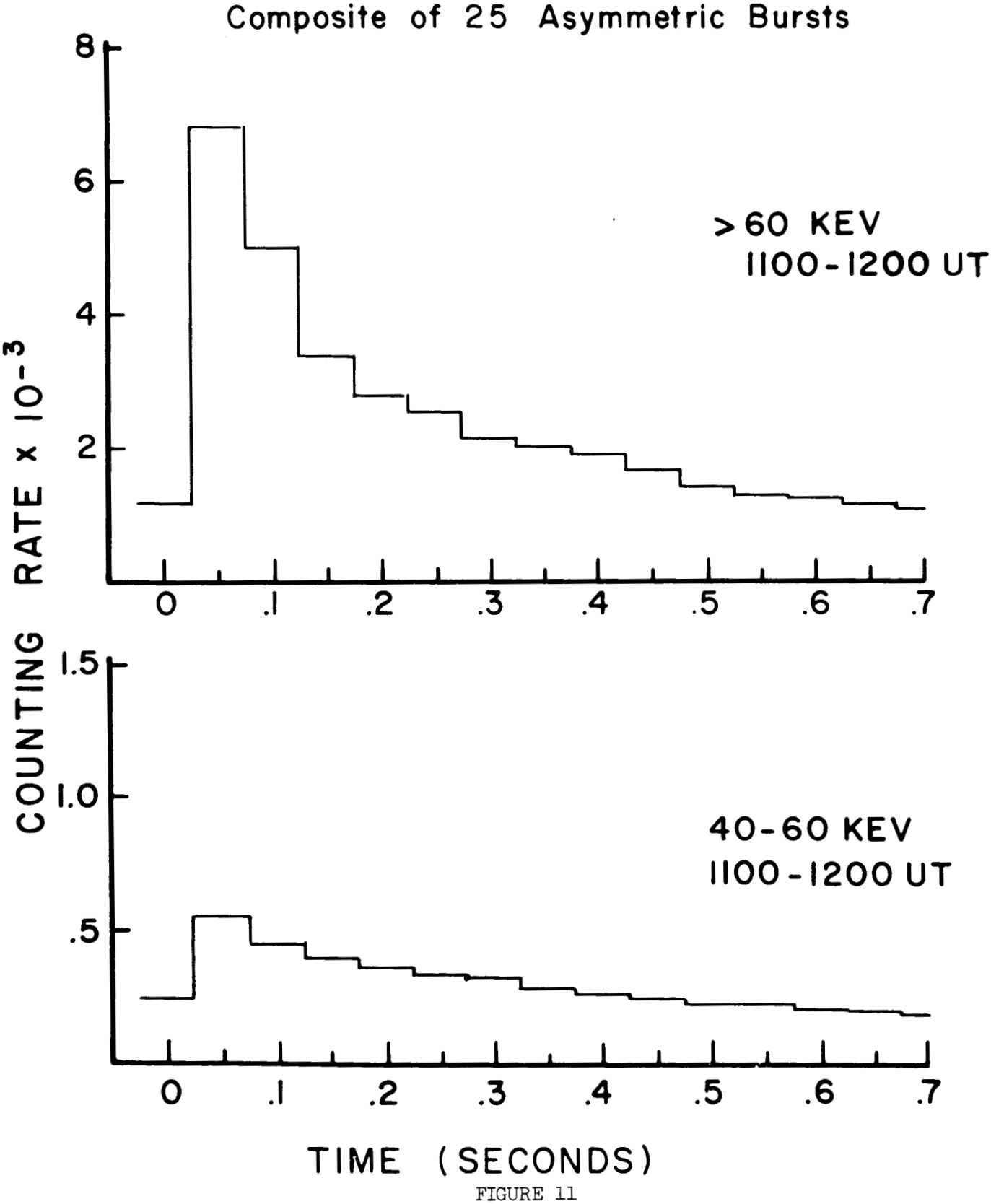
Composite of 25 Asymmetric Bursts
8
6
4
2
>60 KEV
1100-1200 UT
0
.1
.2
.3
.4
.5
.6
.7
COUNTING RATE x 10⁻³
1.5
1.0
.5
40-60 KEV
1100-1200 UT
0
.1
.2
.3
.4
.5
.6
.7
TIME (SECONDS)

FIGURE 11

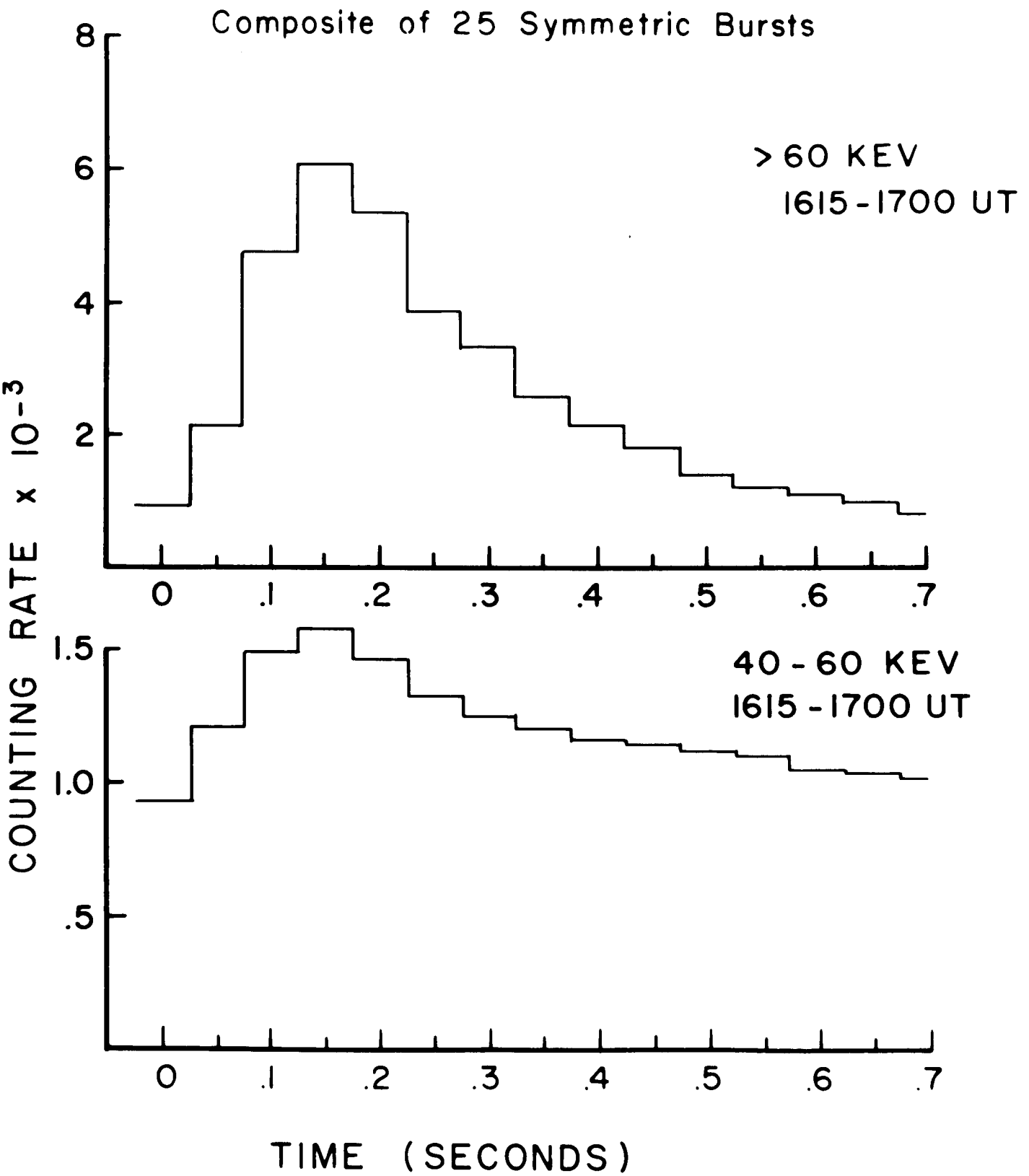
Composite of 25 Symmetric Bursts
> 60 KEV
1615 - 1700 UT
40 - 60 KEV
1615 - 1700 UT
COUNTING RATE x 10⁻³
8
6
4
2
1.5
1.0
.5
0
.1
.2
.3
.4
.5
.6
.7
TIME (SECONDS)

FIGURE 12

UNCLASSIFIED
Security Classification

DOCUMENT CONTROL DATA - R&D

(Security classification of title, body of abstract and indexing annotation must be entered when the overall report is classified)

1. ORIGINATING ACTIVITY *(Corporate author)*

University of Iowa
Department of Physics and Astronomy

2a. REPORT SECURITY CLASSIFICATION
UNCLASSIFIED

2b GROUP

3. REPORT TITLE

Microburst Phenomena 1. Auroral Zone X-rays

4. DESCRIPTIVE NOTES *(Type of report and inclusive dates)*
Progress August 1967

5. AUTHOR(S) *(Last name, first name, initial)*

Venkatesan, D., Oliven, M. N., Edwards, P. J., McCracken, K. G., Steinbock, M.

6. REPORT DATE	7a. TOTAL NO. OF PAGES	7b. NO. OF REFS
August 1967	36	10

8a. CONTRACT OR GRANT NO.	9a. ORIGINATOR'S REPORT NUMBER(S)
Nonr 1509(06)	U. of Iowa 67-18
b. PROJECT NO.	
c.	9b. OTHER REPORT NO(S) *(Any other numbers that may be assigned this report)*
d.	

10. AVAILABILITY/LIMITATION NOTICES

Distribution of the document is unlimited.

11. SUPPLEMENTARY NOTES	12. SPONSORING MILITARY ACTIVITY
	Office of Naval Research

13. ABSTRACT

(see next page)

DD FORM 1 JAN 64 1473

UNCLASSIFIED
Security Classification

14. KEY WORDS	LINK A		LINK B		LINK C	
	ROLE	WT	ROLE	WT	ROLE	WT
Microburst Phenomena						
Microburst Phenomena 1. Auroral Zone X-Rays						
Balloon Observed Auroral Zone Bremsstrahlung X-Rays						
Auroral Zone Precipitation						

INSTRUCTIONS

1. ORIGINATING ACTIVITY: Enter the name and address of the contractor, subcontractor, grantee, Department of Defense activity or other organization *(corporate author)* issuing the report.

2a. REPORT SECURITY CLASSIFICATION: Enter the overall security classification of the report. Indicate whether "Restricted Data" is included. Marking is to be in accordance with appropriate security regulations.

2b. GROUP: Automatic downgrading is specified in DoD Directive 5200.10 and Armed Forces Industrial Manual. Enter the group number. Also, when applicable, show that optional markings have been used for Group 3 and Group 4 as authorized.

3. REPORT TITLE: Enter the complete report title in all capital letters. Titles in all cases should be unclassified. If a meaningful title cannot be selected without classification, show title classification in all capitals in parenthesis immediately following the title.

4. DESCRIPTIVE NOTES: If appropriate, enter the type of report, e.g., interim, progress, summary, annual, or final. Give the inclusive dates when a specific reporting period is covered.

5. AUTHOR(S): Enter the name(s) of author(s) as shown on or in the report. Enter last name, first name, middle initial. If military, show rank and branch of service. The name of the principal author is an absolute minimum requirement.

6. REPORT DATE: Enter the date of the report as day, month, year; or month, year. If more than one date appears on the report, use date of publication.

7a. TOTAL NUMBER OF PAGES: The total page count should follow normal pagination procedures, i.e., enter the number of pages containing information.

7b. NUMBER OF REFERENCES: Enter the total number of references cited in the report.

8a. CONTRACT OR GRANT NUMBER: If appropriate, enter the applicable number of the contract or grant under which the report was written.

8b, 8c, & 8d. PROJECT NUMBER: Enter the appropriate military department identification, such as project number, subproject number, system numbers, task number, etc.

9a. ORIGINATOR'S REPORT NUMBER(S): Enter the official report number by which the document will be identified and controlled by the originating activity. This number must be unique to this report.

9b. OTHER REPORT NUMBER(S): If the report has been assigned any other report numbers *(either by the originator or by the sponsor)*, also enter this number(s).

10. AVAILABILITY/LIMITATION NOTICES: Enter any limitations on further dissemination of the report, other than those imposed by security classification, using standard statements such as:

(1) "Qualified requesters may obtain copies of this report from DDC."

(2) "Foreign announcement and dissemination of this report by DDC is not authorized."

(3) "U. S. Government agencies may obtain copies of this report directly from DDC. Other qualified DDC users shall request through _____."

(4) "U. S. military agencies may obtain copies of this report directly from DDC. Other qualified users shall request through _____."

(5) "All distribution of this report is controlled. Qualified DDC users shall request through _____."

If the report has been furnished to the Office of Technical Services, Department of Commerce, for sale to the public, indicate this fact and enter the price, if known.

11. SUPPLEMENTARY NOTES: Use for additional explanatory notes.

12. SPONSORING MILITARY ACTIVITY: Enter the name of the departmental project office or laboratory sponsoring *(paying for)* the research and development. Include address.

13. ABSTRACT: Enter an abstract giving a brief and factual summary of the document indicative of the report, even though it may also appear elsewhere in the body of the technical report. If additional space is required, a continuation sheet shall be attached.

It is highly desirable that the abstract of classified reports be unclassified. Each paragraph of the abstract shall end with an indication of the military security classification of the information in the paragraph, represented as *(TS), (S), (C), or (U)*.

There is no limitation on the length of the abstract. However, the suggested length is from 150 to 225 words.

14. KEY WORDS: Key words are technically meaningful terms or short phrases that characterize a report and may be used as index entries for cataloging the report. Key words must be selected so that no security classification is required. Identifiers, such as equipment model designation, trade name, military project code name, geographic location, may be used as key words but will be followed by an indication of technical context. The assignment of links, roles, and weights is optional.

ABSTRACT

High-time resolution x-ray equipment flown from Ft. Churchill, Manitoba, Canada on August 11, 1965 provides evidence for species of auroral zone x-ray microbursts with an asymmetric time profile. These asymmetric microbursts are characterized by a rise of the form $1 - e^{-t/\tau_R}$ where τ_R is about 30 milliseconds, and a decay of the form of e^{-t/τ_D} where τ_D is about 200 milliseconds, and a typical peak flux for the largest events of J_o ($E_{x\text{-ray}} > 60$ keV) $\sim 10^2$ photons cm^{-2} sec^{-1} at 10 g/cm^2. An episode of these asymmetric bursts was observed in the early morning hours (after 4:30 local time) and an episode of the more common symmetric microbursts began after 9:30 local time. The fast rise times, and the lack of dispersion $\gtrsim 10$ milliseconds in the x-ray bursts observed at different energies implies restrictions on the nature, and propagation of the parent electron microbursts.